

# Pre-processing for Muscle Motion Analysis: Adaptive Guided Image Filtering for Speckle Reduction of Ultrasound Images

Ye Chen<sup>1,2,3</sup>, Yongjin Zhou<sup>1,2,\*</sup>, Kamen Ivanov<sup>1,2</sup>, Jizhou Li<sup>1,2</sup>, Yuanzhong Shu<sup>3</sup>, Lei Wang<sup>1,2</sup>

**Abstract**— Skeletal muscle is an important tissue of human body, and its contractions control and regulate body motions. Muscle contraction results in morphological changes of the related muscles. Ultrasound imaging is an effective tool for studying muscle architectures and monitoring the morphological changes of muscles. The latter process can be realized with a motion estimation algorithm. However, ultrasound images are usually corrupted by speckle noises and performance of motion estimation methods can be significantly affected by the noises. To get a better performance in motion analysis, in this paper, as a pre-processing step, an adaptive filter named *adaptive guided image filtering* (AGF) is suggested to reduce speckle noises. We first transformed the multiplicative noise model into an additive one by taking the logarithm of the original speckled data, then performed AGF to obtain the filtered image, and finally took the tackled image back into exponent. Experimental results showed that AGF had a better performance in terms of noise attenuation and edge preservation compared with other standard filters. In quantitative results, the filtered images also had the highest Peak-Signal-to-Noise Ratio (PSNR) using AGF. It's believed that AGF is a good choice for the pre-processing stage of muscle motion analysis.

**Index Terms**—Ultrasound image, speckle reduction, adaptive guided image filtering, muscle motion, optical flow

## I. INTRODUCTION

Skeletal muscle is an important tissue of human body, and its contractions control and regulate body motions. The skeletal muscle architecture is a primary determinant of muscle functions [1]. Since mechanical properties of muscles strongly depend on their architecture, muscle architecture can be used to characterize muscle activities. Ultrasound imaging is an effective tool for detecting and measuring muscle architectures [2], such as muscle thickness [3], pennation angle [4, 5] and cross-sectional area [6, 7] during isometric and dynamic contractions since it is economical, comparatively safe and adaptable. Muscle contraction not only causes muscle motions, but also results in morphological changes. Different contractions could result in different morphological changes. Therefore, it is natural to estimate muscle mobility functions by monitoring the morphological changes of muscle in ultrasound image sequence [8, 9]. This process can be tracked with a motion estimation algorithm such as optical flow [8, 9] or image registration.

However, the performance of these methods is closely related to the image quality, and one of the ultrasound image shortcomings is the poor image quality, affected by speckle noise. Speckle noise affects all coherent imaging systems especially medical ultrasound ones. Within each resolution cell a number of elementary scatters reflect the incident wave towards the sensor. The backscattered coherent waves with different phases undergo a constructive or a destructive interference in a random manner. The acquired image is thus corrupted by a random granular pattern called “speckle” that delays the interpretation of the image content. Speckle noise, which can be considered as a kind of multiplicative noise [10], degrades the quality of ultrasonic images. It reduces the ability to distinguish fine details and hence decreases the accuracy of motion analysis. Accordingly, speckle filtering is a central pre-processing step for motion analysis.

As we know, adaptive filters take a moving filter window and estimate the statistical information of all pixels' grey value, such as the local mean and the local variance. The central pixel's output value is dependent on the statistical information. Adaptive filters adapt themselves to the local texture information surrounding a central pixel in order to calculate a new pixel value. Adaptive filters behave much better than low-pass smoothing filters in preservation of the image sharpness and details while suppressing the speckle noise [11]. In literature, the most widely cited and applied filters in speckle reduction include the Lee [12], Frost [13], Kuan [14], wiener [15] and median filters [16]. These filters have an obvious superiority compared to low pass filters, since they take into account the local statistical properties of the image. More recently, some state-of-the-art techniques have been proposed to reduce the speckle noise, such as speckle reducing anisotropic diffusion [17], rayleigh-maximum-likelihood filtering [18], and speckle reducing bilateral filtering (SRBF) [19].

In this paper, we applied an adaptive filter named *adaptive guided image filtering* (AGF) [20] to reduce speckle noises. It is reported that this method is able to perform halo-free edge slope enhancement simultaneously with the noise reduction [20]. Compared with other filters, the results from experiments using the suggested method showed a better performance on noise attenuation in background and smooth regions and enhancement in edge areas. Finally, we used the filtered images for muscle motion analysis and evaluated the improvement after filtering using AGF.

\*Corresponding author: yj.zhou@siat.ac.cn.

1. The Shenzhen Key Laboratory for Low-cost Healthcare, China  
2. Shenzhen Institutes of Advanced Technology, Chinese Academy of Sciences, China  
3. School of Information Engineering, Nanchang Hangkong University, China

## II. METHODS

AGF is based on guided image filtering (GIF) [21] and the shift-variant technique, part of adaptive bilateral filtering (ABF) [22]. In this section, we will review the method briefly and more details about it can be found in [20-23].

### A. Adaptive Guided Image Filtering

It has been proven that AGF has good edge-preserving characteristic as described in [20]. The filtering process of AGF is originally done under the guidance of an image  $G$  that can be either the input image  $I$  or another image. We first express AGF in terms of the filter kernel. Let  $I_p$  and  $G_p$  denote the intensity value at pixel  $p$  of the input image and the guide image, respectively.  $w_k$  denotes the kernel window centered at pixel  $k$ . AGF is then formulated as:

$$AGF(I)_p = \sum_{q \in w_k} W_{AGF_{pq}}(G) I_q, \quad (1)$$

where the kernel weight function  $W_{AGF_{pq}}(G)$  can be expressed by:

$$W_{AGF_{pq}}(G) = \frac{1}{|w|} \sum_{k:(p,q) \in w_k} \left( 1 + \frac{(G_p + \varepsilon_p) - \mu_k)(G_q - \mu_k)}{\sigma_k^2 + \varepsilon} \right) \quad (2)$$

where  $\mu_k$  and  $\sigma_k^2$  are the mean and variance of the guide image  $G$  in local window  $w_k$ ,  $|w|$  is the number of pixels in this window,  $\varepsilon_p$  is the added offset and  $\varepsilon$  is the smoothing parameter. An offset-choosing strategy is also applied in AGF, in the same manner as this done in the ABF [22, 23]. That is:

$$\varepsilon_p = \begin{cases} MAX(w_k) - G_p & \text{if } \Delta_p > 0 \\ MIN(w_k) - G_p & \text{if } \Delta_p < 0 \\ 0 & \text{if } \Delta_p = 0 \end{cases}, \quad (3)$$

where the intensity difference is defined by  $\Delta_p = G_p - \mu_k$ .

The key to understand the edge-preserving ability of AGF lies in the term  $\left( 1 + \frac{((G_p + \varepsilon_p) - \mu_k)(G_q - \mu_k)}{(\sigma_k^2 + \varepsilon)} \right)$  of equation (2). When both  $(G_p + \varepsilon_p)$  and  $G_q$  are concurrent on the same side of an edge (smaller or larger than the mean), the weight assigned to pixel  $q$  is large. Conversely, a small weight will be assigned to pixel  $q$  when they are on different sides (one is smaller and one is larger than the mean). The degree of smoothing of AGF is adjusted via parameter  $\varepsilon$ . The larger the value of  $\varepsilon$  is, the smoother the filtered image will be [20].

### B. Image De-noising and Application Procedure

The main process of this algorithm is as follows:

- Transform the multiplicative noise model into an additive one by taking the logarithm of the original

speckled data.

- For each input image perform an AGF to obtain the corresponding filtered image.
- Take an exponent.
- Use the de-noised images for muscle motion estimation.

## III. EXPERIMENTAL RESULTS & DISCUSSIONS

The experiments were performed on a continuous sequence of quadriceps muscle images taken during a contraction process. The sequence consisted of 240 images in total. A real-time B-mode ultrasonic scanner (EUB-8500, Hitachi Medical Corporation, Tokyo, Japan) provided with an electronic linear array probe (L53L, Hitachi Medical Corporation, Tokyo, Japan) was used to obtain transactional ultrasound images of the quadriceps muscle. A human subject ethical approval was obtained from the relevant committee in the Hong Kong Polytechnic University before carrying out the experiment. Details of the experimental setup can be found in [24]. Here is evaluated the speckle noise reduction performance of the AGF when it is used for pre-processing in muscle motion analysis. The AGF is compared to ABF, mean, median and wiener filters, respectively. The guide image  $G$  and the original image  $I$  of AGF were chosen to be identical. In all cases, the moving window size was empirically set to  $7 \times 7$ . All the source code, prepared to demonstrate the current work, was written in Matlab 7.11 (Mathworks, Inc., Massachusetts, USA).

A representative original muscle image was used in this evaluation. The image is shown in Fig.1 (a). It was processed using the ABF, mean, median, wiener and AGF filters, respectively. The corresponding results are shown in Fig.1 (b)-(f). In this example, the  $\varepsilon$  parameter is set to a constant  $\varepsilon = 0.04$  in AGF, the  $\sigma_s$  and  $\sigma_r$  are set to 3 and 0.3 in ABF, respectively. Note that the mean filter provides good noise attenuation and smoothing, but in its output the edges are significantly smoothed. The median filter suppresses the noise slightly better than mean filter in uniform areas, at the cost of excessive smoothing of details, which is especially apparent in the mean filter output. The wiener filter output is effective in noise suppression with better edge preservation quality than the mean and median filter outputs. The ABF filter output also provides a better performance than the above-mentioned three filters in the sense of noise suppression and gradient preservation. It is clear from the images that AGF provides the best performance in terms of noise suppression and image detail preservation among the tested algorithms.

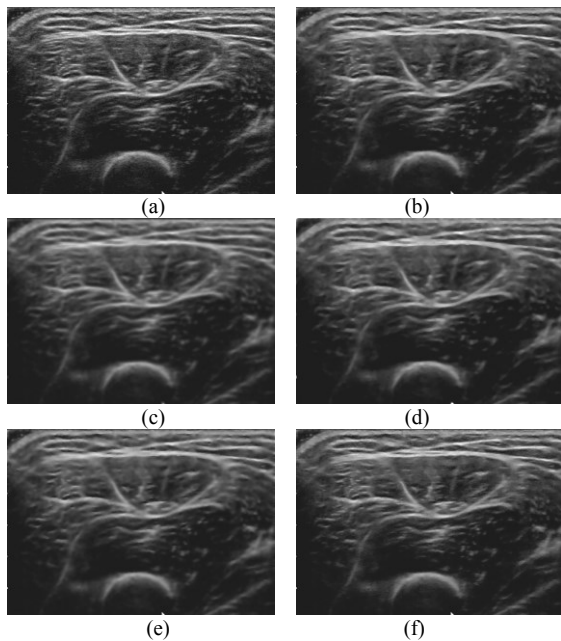


Fig.1. Muscle image de-speckling: (a) Original image and processed with (b) ABF ( $\sigma_s=3$ ,  $\sigma_r=0.3$ ), (c) mean, (d) median, (e) wiener and (f) AGF ( $\mathcal{E}=0.04$ ) filters.

To further evaluate the output from each filter, consider a single scan line running through the image as shown in Fig.2 (a). Fig.2 (b) shows the gray level along the line of the original ultrasound image and the corresponding outputs from the ABF, mean, median, wiener and AGF filters. An examination of the scan line shows that the mean, median and wiener filter outputs appear almost noise-free at the cost of significant loss of sharp-transition details. The ABF and AGF filters strike a better balance between noise attenuation and detail preservation.

In addition to the subjective visual results, Peak-Signal-to-Noise Ratio (PSNR) is utilized in our experiments to measure the effectiveness of different algorithms quantitatively. The metric is calculated for the ultrasound muscle sequence. PSNR is defined as:

$$PSNR = 10 \log_{10} \left( \frac{255}{MSE} \right), \quad (4)$$

$$MSE = \frac{1}{MN} \sum_{i=1}^M \sum_{j=1}^N (X(i, j) - Y(i, j))^2, \quad (5)$$

where  $X, Y$  represent the original and the de-noised images, respectively.

Fig.3 demonstrates the PSNR of experimental results for the different methods. It can be observed from Fig.3 that AGF has the highest PSNR, followed by the ABF, wiener, median and mean filters, respectively. It can be clearly seen that the mean filter provides the worst noise attenuation, while the median filter outperforms the mean filter under the same criterion. The wiener filter provides better noise attenuation than the mean and median filters. The ABF filter provides better results than the mean, median and wiener filters in term of the metric. The AGF filter provides the best performance among the tested algorithms.

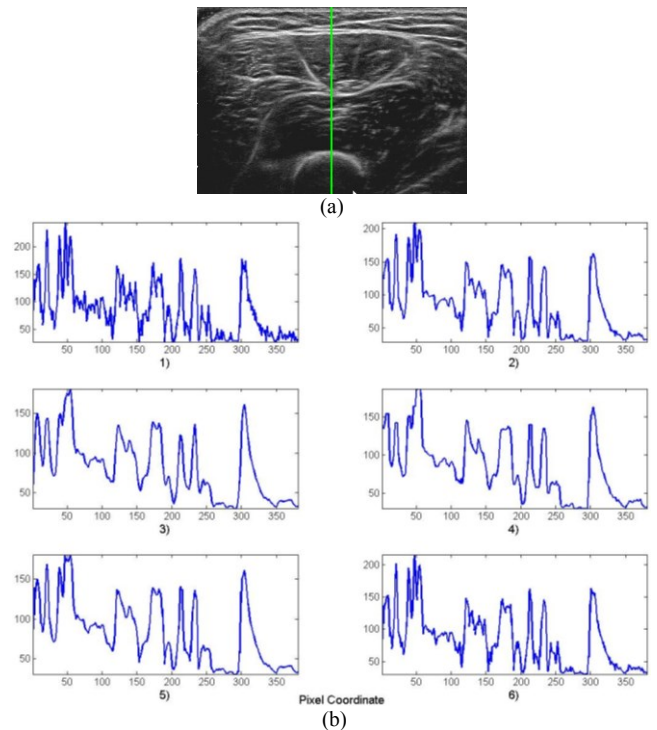


Fig.2. The original image and the scan line are depicted in (a). The 277<sup>th</sup> column of the original and processed ultrasound images in Fig.1 are depicted in (b). 1) Original ultrasound image, 2) ABF ( $\sigma_s=3$ ,  $\sigma_r=0.3$ ), 3) mean, 4) median, 5) wiener and 6) AGF ( $\mathcal{E}=0.04$ ) filter outputs.

Finally, we used the original and de-noised images for muscle motion analysis. Fig.4 (a)-(f) show the results of optical flow processing [9] without filtering and using ABF, mean, median, wiener, AGF filters, respectively. Based on visual motion inspection criteria [25], it can be clearly seen that the result using AGF is better than results obtained without pre-processing or those obtained using the other four methods.

#### IV. CONCLUSION

In this paper, we explored the performance of adaptive guided image filtering for speckle noise reduction in ultrasound images in the context of its application as a pre-processing stage in muscle motion analysis. The method outperforms the ABF, mean, median and wiener filters that are used for comparison. By visual inspection, it is evident that AGF strikes the balance between noise attenuation and detail preservation. In terms of quantitative results, AGF demonstrated the highest PSNR compared to the other four filters. It can be clearly seen that AGF is a good choice for the pre-processing stage in muscle motion analysis.

#### ACKNOWLEDGMENT

The project is supported partially by the Hong Kong Innovation and Technology Commission (GHP/047/09), the National 863 Program of China (2012AA02A604), the National 973 Program of China (2010CB732606), the next generation communication technology Major project of National S&T (2013ZX03005013), the 'Low-cost

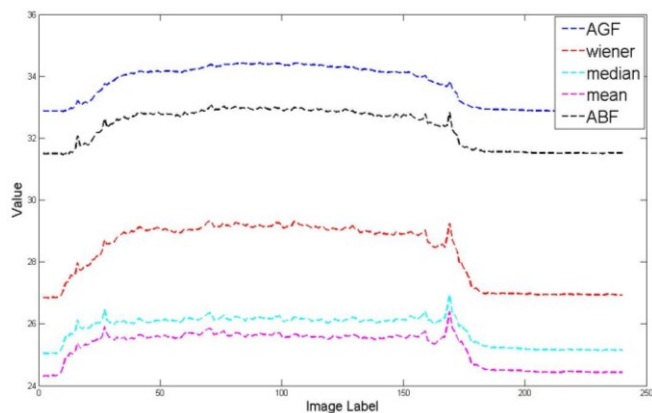


Fig.3. Comparison chart of PSNR of different methods for ultrasound sequence.

Healthcare' Programs of Chinese Academy of Sciences, the Guangdong Innovative Research Team Program (2011S013, GRTF-LCHT), International Science and Technology Cooperation Program of Guangdong Province (2012B050200004). Shenzhen outstanding youth fund (JC201005280467A).

#### REFERENCES

- [1] R. L. Lieber. (2002). *Skeletal Muscle Structure, Function, and Plasticity: The Physiological Basis of Rehabilitation*.
- [2] P. W. Hodges, L. H. M. Pengel, R. D. Herbert, and S. C. Gandevia, "Measurement of muscle contraction with ultrasound imaging," *Muscle & Nerve*, vol. 27, pp. 682-692, 2003.
- [3] J. Shi, Y. P. Zheng, X. Chen, and Q. H. Huang, "Assessment of muscle fatigue using sonomyography: Muscle thickness change detected from ultrasound images," *Medical Engineering & Physics*, vol. 29, pp. 472-479, 5 2007.
- [4] Y. J. Zhou, J. Z. Li, G. Q. Zhou, and Y. P. Zheng, "Dynamic measurement of pennation angle of gastrocnemius muscles during contractions based on ultrasound imaging," *Biomedical engineering online*, vol. 11, p. 63, 2012.
- [5] Y. J. Zhou and Y. P. Zheng, "Estimation of muscle fiber orientation in ultrasound images using revolving hough transform (RVHT)," *Ultrasound in medicine & biology*, vol. 34, pp. 1474-1481, 09, 2008.
- [6] C. N. Maganaris, V. Baltzopoulos, and A. J. Sargeant, "Human calf muscle responses during repeated isometric plantarflexions," *Journal of biomechanics*, vol. 39, pp. 1249-1255, 2006.
- [7] N. D. Reeves, C. N. Maganaris, and M. V. Narici, "Ultrasonographic assessment of human skeletal muscle size," *European journal of applied physiology*, vol. 91, pp. 116-118, 01, 2004.
- [8] J. Shi, J. Y. Guo, S. X. Hu, and Y. P. Zheng, "Recognition of finger flexion motion from ultrasound image: a feasibility study," *Ultrasound Med Biol*, vol. 38, pp. 1695-704, Oct 2012.
- [9] J. Z. Li and Y. Zhou, "Estimation of Longitudinal Muscle Motion using a Primal-dual Algorithm," in *the 5th Biomedical Engineering International Conference (BMEiCON-2012)*, 2012.
- [10] C. B. Burckhardt, "Speckle in ultrasound B-mode scans," *IEEE Transactions on Sonics and Ultrasonics*, vol. 25, pp. 1-6, 1978.
- [11] X. Zong, A. F. Laine, and E. A. Geiser, "Speckle reduction and contrast enhancement of echocardiograms via multiscale nonlinear processing," *IEEE Transactions on Medical Imaging*, vol. 17, pp. 532-540, 1998.
- [12] J. S. Lee, "Speckle suppression and analysis for synthetic aperture radar," *Opt. Eng.*, vol. 25, pp. 636-643, 1986.
- [13] V. S. Frost, J. A. Dites, K. S. Shanmugan, and J. C. Holtzman, "A model for radar images and its application to adaptive digital filtering for multiplicative noise," *IEEE Trans. Pattern Anal. Machine Intell.*, vol. PAMI-4, pp. 157-165, 1982.

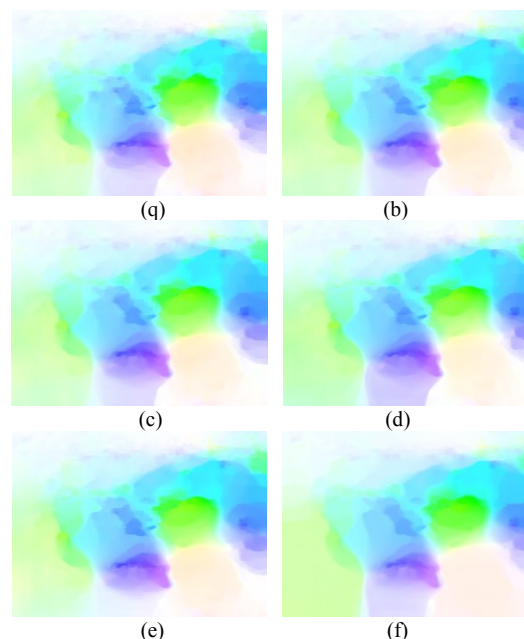


Fig.4. Optical flow estimation by the different methods: (a) original, (b) ABF, (c) mean, (d) median, (e) wiener, (f) AGF.

- [14] D.T.Kuan, A. A. Sawchuk, T. C. Strand, and P. Chavel, "Adaptive restoration of images with speckle," *IEEE Trans. Acoust., Speech, Signal Process.*, vol. ASSP-35, pp. 373-383, 1987.
- [15] D.Hillery, "Iterative wiener filters for Images restoration," *IEEE Transaction on SP* vol. 39, pp. 1892-1899, 1991.
- [16] T. Loupas, W. N. Medichen, and P. L. Allen, "An adaptive weighted median filter for speckle suppression in medical ultrasound images," *IEEE Trans. Circuits Syst.*, vol. 36, pp. 129-135, 01, 1989.
- [17] Y. Yu and S. T. Acton, "Speckle reducing anisotropic diffusion," *IEEE Transactions on Image Processing*, vol. 11, pp. 1260-1270, 2002.
- [18] T. C. Aysal and K. E. Barner, "Rayleigh-Maximum-Likelihood Filtering for Speckle Reduction of Ultrasound Images," *IEEE Transactions On Medical Imaging*, vol. 26, pp. 712-727, 05, 2007.
- [19] S. Balocco, C. Gatta, O. Pujol, J. Mauri, and P. Radeva, "SRBF: Speckle reducing bilateral filtering," *Ultrasound Med Biol*, vol. 36, pp. 1353-63, Aug 2010.
- [20] C. C. Pham, S. V. U. Ha, and J. W. Jeon, "Adaptive Guided Image Filtering for Sharpness Enhancement and Noise Reduction," *PSIVT*, pp. 324-34, 2011.
- [21] K. He, J. Sun, and X. Tang, "Guided Image Filtering," in *Proc. Eur. Conf. Comput. Vis.*, pp. 1-14, 2010.
- [22] B. Zhang and j. P. Allebach, "Adaptive Bilateral Filter for Sharpness Enhancement and Noise Removal," in *Proc. Intl. Conf. on Image Processing (ICIP)*, 2007.
- [23] B. Zhang and j. P. Allebach, "Adaptive bilateral filter for sharpness enhancement and noise removal," *IEEE Transaction on Image Processing*, vol. 17, pp. 664-678, 2008.
- [24] X. Chen, Y. P. Zheng, J. Y. Guo, Z. Zhu, S. C. Chan, and Z. Zhang, "Sonomyographic responses during voluntary isometric ramp contraction of the human rectus femoris muscle," *Eur J Appl Physiol*, vol. 112, pp. 2603-14, Jul 2012.
- [25] C. Liu, W. T. Freeman, E. H. Adelson, and Y. Weiss, "Human-assisted motion annotation," in *IEEE Conference on Computer Vision and Pattern Recognition CVPR*, 2008.